



RESEARCH ARTICLE

Integrative probabilistic design of river jetties by 3D numerical models of transport phenomena: The case study of Kabakoz River jetties

Arif Uğurlu^{1*}  • Can Elmar Balas¹ 

¹ General Directorate of Infrastructure Investments, Ministry of Transport and Infrastructure, Ankara, Türkiye

² Gazi University, Faculty of Engineering, Civil Engineering Department, Sea and Aquatic Sciences Application and Research Center, Ankara, Türkiye

ARTICLE INFO

Article History:

Received: 03.01.2024

Received in revised form: 02.04.2024

Accepted: 15.05.2024

Available online: 24.06.2024

Keywords:

Coastal structures

HYDROTAM-3D

Marine engineering

Monte Carlo simulation

Probabilistic design

Wave transformation

ABSTRACT

Various methods are employed to investigate the effects of coastal structures in coastal areas on marine environments and transport phenomena. These methods can be categorized into physical models and numerical simulations. Due to the lack of long-term wave height data in Türkiye, numerical models are utilized to estimate wave heights generated by wind based on long-term measured wind speeds. These wave heights generated in deep sea conditions can be transported to the coast by wave transformation and interactions between coastal structures and waves, turbulence, currents induced by wind and breaking waves, coastal sediment transport rates, and changes in the coastline can be successfully predicted with the assistance of numerical models. In the scope of this study, the new “Integrative Probabilistic Design Approach of River Jetties” was developed. 3D numerical models were used for the optimum design, considering the sediment transport near the jetties and aiming to protect the coastal environment in the long term. 3D numerical modeling has been conducted to investigate the transport phenomena occurring at the outlet of the Kabakoz River in the Şile District of İstanbul Province to acquire the optimum layout and design of the coastal structures. The study presents the “Integrative Probabilistic Design Approach” for coastal protection structures by wind and wave climate, wave transformation, coastal sediment transport, shoreline change, and coastal structure probabilistic design sub-models. Monte Carlo Simulation of Hudson Limit State function conducts probabilistic design for the jetties. The greatest advantage of probabilistic design (Monte Carlo Simulation) is the prediction of uncertainties, such as wave height changes under design conditions. Following the completion of the construction of groins, the effect of probabilistic design on both design and coastal morphology can be evaluated precisely. In conclusion, in the study area, 146,237.55 m³ of sediment is transported annually from west to east and 221,043.49 m³ from east to west. In the absence of coastal structures, sediment transport from east to west is approximately 1.5 times greater than from west to east. The annual net coastal sediment transport from east to west is approximately 74,805.94 m³, while the total transport is estimated to be 367,281.04 m³. The coastline is expected to reach sediment balance within approximately two years. In this study, the coastal structure of a jetty is designed from an innovative probabilistic design

* Corresponding author

E-mail address: arif.ugurlu@uab.gov.tr (A. Uğurlu)



perspective. The aim is to ensure the reliability of the structure and, at the same time, protect the morphology of the coastline where the structure will be constructed. The region's wind and wave climate were initially determined using Hydrotam 3D software. Following this procedure, the length of the jetty is predicted considering the closure depth. The model parameters were calibrated from coastline morphology using satellite images and Google Earth over the past twenty years. These parameters are defined to Hydrotam 3D as input data; a trial-and-error model application procedure calibrates the coastline's accumulation and erosion. Finally, the probabilistic design is conducted with Monte Carlo Simulation using the Hudson Equation as the limit state function. Det Norske Veritas developed a design code for marine structures in 1992, where the target reliability is 10^{-3} for structures with less serious failure consequences. This reliability level validated the Level IV model presented in this paper. The class of failure depends on the possibility of timely warning, and these standards can be revised by the model presented to address the effects of climate change on the design of maritime structures.

Please cite this paper as follows:

Uğurlu, A., & Balas, C. E. (2024). Integrative probabilistic design of river jetties by 3D numerical models of transport phenomena: The case study of Kabakoz River jetties. *Marine Science and Technology Bulletin*, 13(2), 151-167. <https://doi.org/10.33714/masteb.1414048>

Introduction

The study area covers the coastal area of Kabakoz Beach, located in Şile District, Istanbul Province, as shown in Figure 1 and Figure 2.



Figure 1. Geographic location of the study area (Google Earth, 2023)



Figure 2. Location of study area (Google Earth, 2023)

Lima et al. (2020) determined the length of the jetty, considering the changes in coastal morphology but ignoring the design procedure of the jetty.

An erosion study conducted by Roebeling et al. (2018) on the central Portuguese coast includes economic design circumstances by focusing on coastal morphology evaluation but not the structure's design. Various coastal structures were compared for their effects on coastal morphology by Franzen et al. (2021) but the design method directly affecting morphology was not considered. The effects of Pranburi Jetties on the coastal area, which take place in Pranburi River Inlet located on the western coast of the Gulf of Thailand, were studied by Phanomphongphaisarn et al. (2020). The one-line model was used to obtain the results by focusing on coastal erosion and ignoring the design methodology and advantages of a 3D model. The shoreline change on North Java Beach with groin protection was investigated by Setyandito et al. (2020), concentrating on morphology effects but ignoring the design conditions of the system. As seen from the studies in the literature, there is a gap for an integrated approach for marine structures fulfilled by this study. This study aims to develop a methodology to revise the design standards by examining the effects of climate change.

Material and Methods

To determine the wind climate of the study area, hourly wind measurements from the Şile Meteorological Station and 6-hour wind forecasts from the ECMWF (European Centre for Medium-Range Weather Forecasts) operational archive at

coordinates 41.2°N-29.7°E, representing the project area, were compared and analyzed. The comparisons of wind speeds between the common measurement periods and durations of data sources are presented in Figure 3. All presented wind speed measurements and hindcasts are at a height of 10 meters (U10). After the comparison studies, it was concluded that wind predictions over the sea surface for the coordinates 41.2°N-29.7°E from ECMWF between 2000-2021 are consistent with the data from the Şile Meteorological Station. It was decided that these data over the sea surface could be used to determine the wind climate of the coastal area in the project area. Upon examination of the wind roses provided in Figure 4, it is observed that the wind predominantly blows from the northeast (NE) to the east-northeast (ENE) direction, progressing clockwise from the sea. During the winter and spring seasons, the frequency of southwest (SW) winds blowing from the land is observed, while during the summer and autumn seasons, the frequency of northeast (NE) winds tends to increase.

Monthly average and maximum wind speeds are also presented graphically (Figure 5). The monthly averages of wind

speeds were calculated by taking the arithmetic mean of all wind speeds within that month. Monthly maximum values represent the highest, lowest, and average maximum values observed within that month over the same periods (the average of the highest values for each year for any given month).

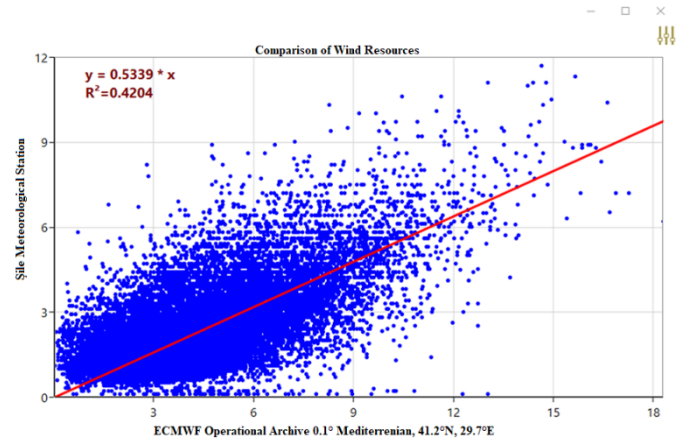


Figure 3. Comparison of wind speeds obtained from Şile Meteorological Station and ECMWF over sea surface Operational Archive at 41.2°N-29.7°E (HYDROTAM-3D, 2023)

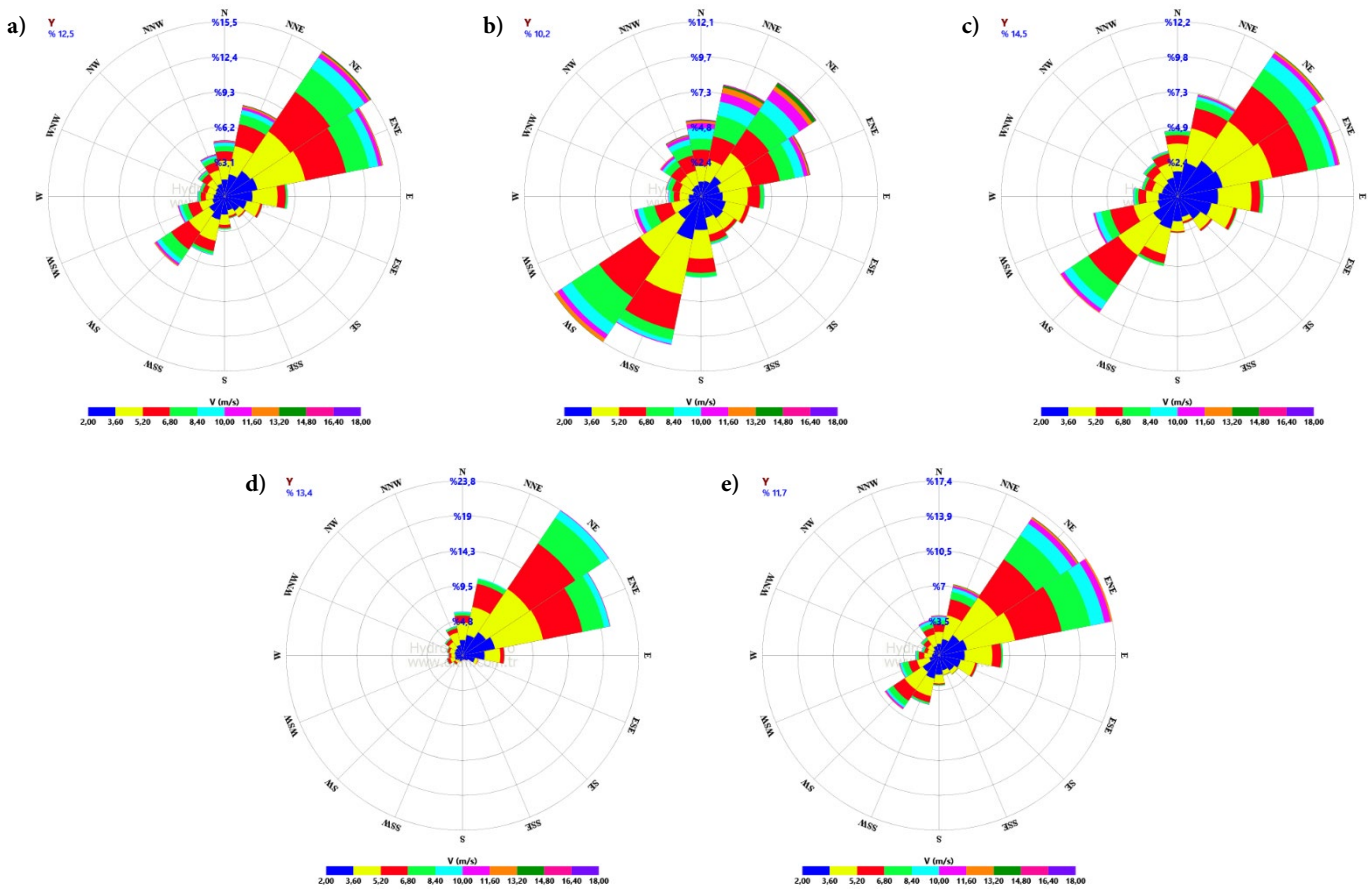


Figure 4. a) Annual and seasonal (b: winter, c: spring, d: summer, e: autumn) wind roses for the ECMWF over the sea surface Operational Archive at coordinates 41.2°N-29.7°E (HYDROTAM-3D, 2023)

The highest wind speeds and prevailing wind directions by year are presented in Figure 6. While the monthly average wind speed ranges from 4 to 5 m/s, the highest maximum wind speeds vary between 12 and 18 m/s. During the study period, the highest wind speed, at 18 m/s, was observed coming from the North (N) direction.

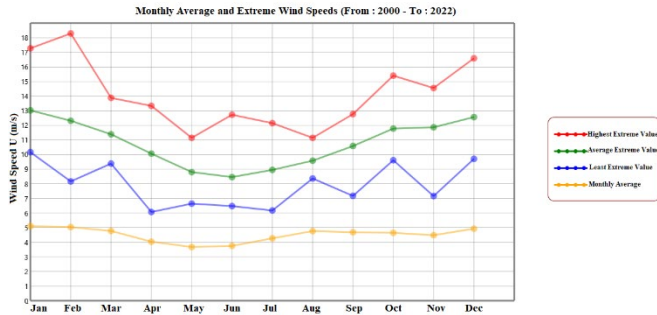


Figure 5. Monthly average and maximum wind speeds based on ECMWF operational archive data at coordinates 41.2°N-29.7°E for 2000-2021 (HYDROTAM-3D, 2023)

In the studied marine area, effective fetch distances (‘fetch’; the length of the sea area extending from one coast to another in the wind direction) have been determined in Figure 7 and presented in Table 1. The cosine-averaging method was applied to determine the effective wave fetch length for all directions. Considering the location of the marine area, the wave fetch distances that could cause the most wave actions are in the North-northeast (NNE) – East-northeast (ENE) direction range.

ECMWF conducts meteorological predictions using its atmospheric numerical model and performs wave predictions with a third-generation wave model called the WAM wave prediction model, one of the most widely used models worldwide. Developed collaboratively by researchers and scientists in the Wave Model Development and Implementation (WAMDI) group, this model aims to provide a wave prediction tool based on physical principles (Wamdi Group, 1988).

Table 1. Effective fetch distances (‘Fetch’) (km)

Direction	Angle (°)	Eff. Fetch (m)
N	0	464930.1
NNE	22.5	581098.8
NE	45	526249
ENE	67.5	674081.9
E	90	72782.8
ESE	112.5	1962.23
SE	135	998.25
SSE	157.5	729.37
S	180	678.33
SSW	202.5	631.11
SW	225	581.32
WSW	247.5	545.65
W	270	17198.6
WNW	292.5	164450.8
NW	315	251326.7
NNW	337.5	320392.6

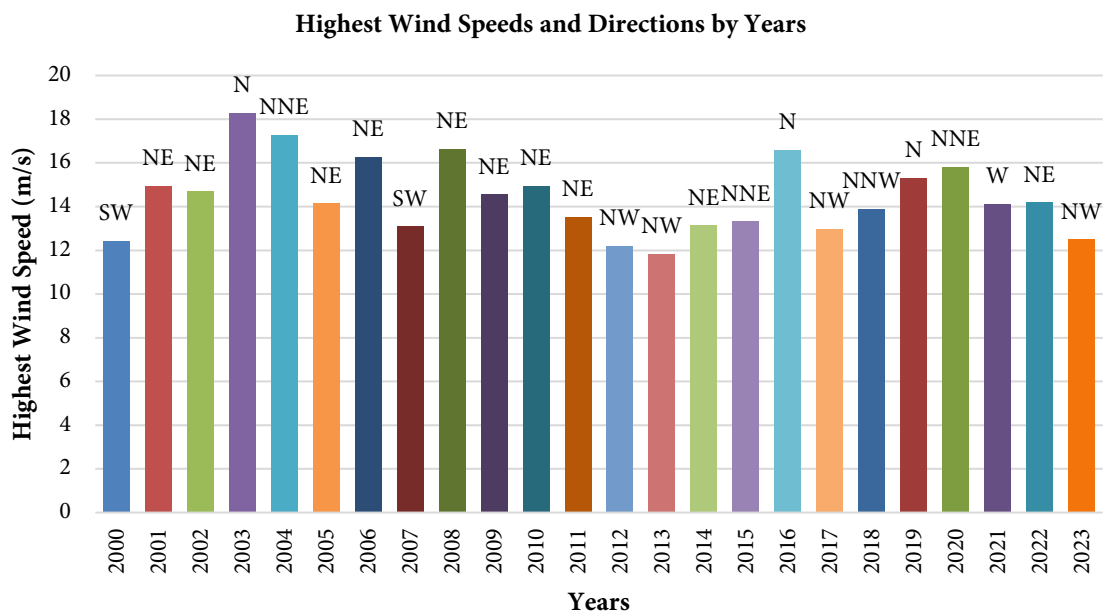


Figure 6. The highest wind speeds and prevailing directions based on ECMWF operational archive data at coordinates 41.2°N-29.7°E for 2000-2021 (HYDROTAM-3D, 2023)

Long-term wave statistics studies were conducted using wave predictions from the ECMWF operational archive for 2000-2022 at the coordinates 41.2°N-29.7°E. The significant wave height (H_s ,12) with a 12 hours per year exceedance probability obtained from long-term wave statistics studies falls within the $1.66 \text{ m} < H_s,12 < 5.47 \text{ m}$. The classification based on wave height in the Coastal Structures Planning and Design Manual of AYGM (2016) corresponds to the effective coastal (E) classification. The model predictions also indicate that the primary directional range is from North (N) to Northeast (NE) in a clockwise direction.

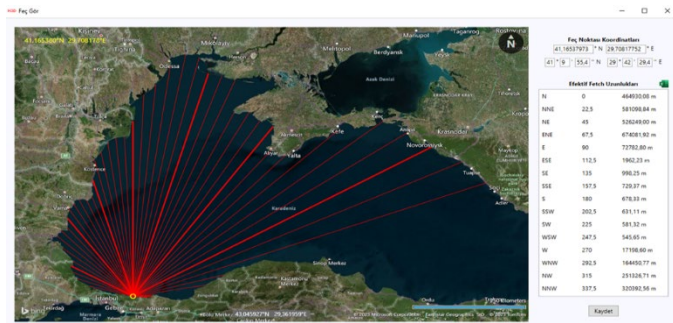


Figure 7. Fetch distances by directions (HYDROTAM-3D, 2023)

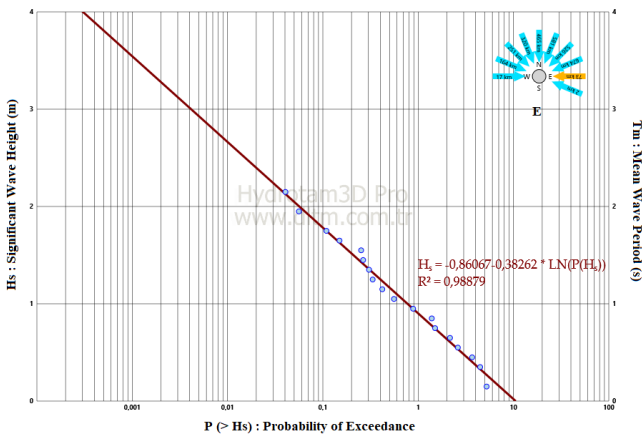


Figure 8. Long-term significant wave statistics for the East (E) direction

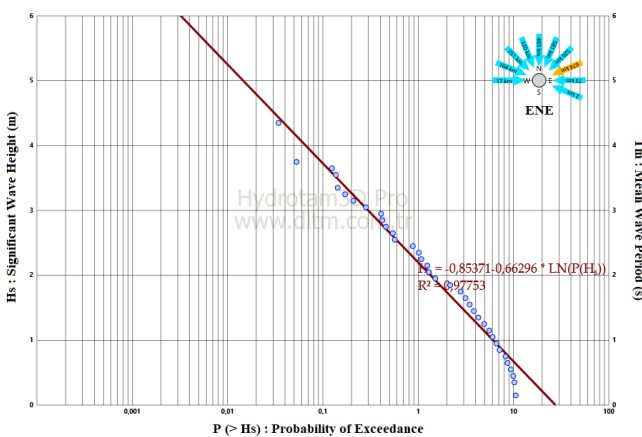


Figure 9. Long-term significant wave statistics for the East-northeast (ENE) direction

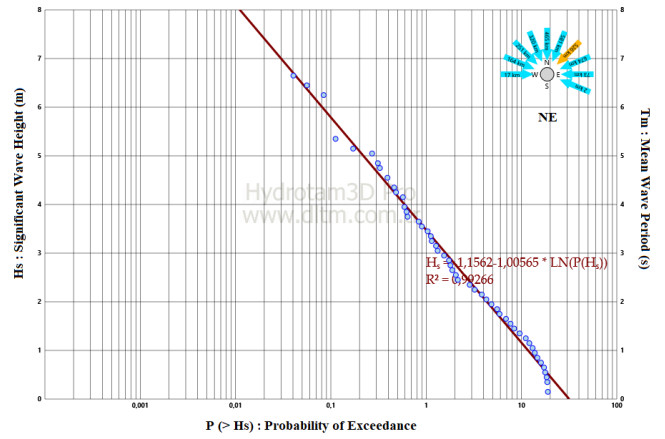


Figure 10. Long-term significant wave statistics for the Northeast (NE) direction

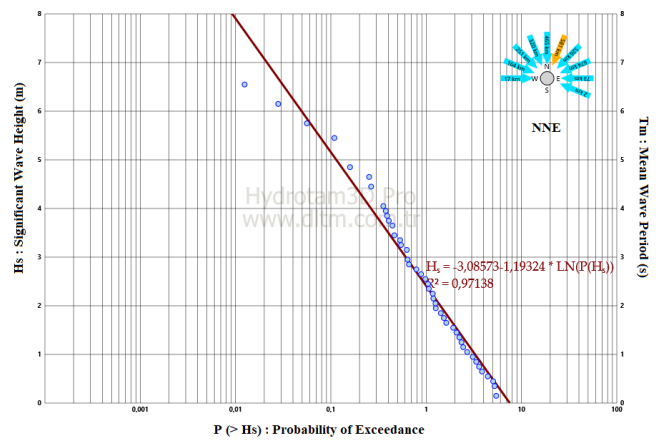


Figure 11. Long-term significant wave statistics for the North-northeast (NNE) direction

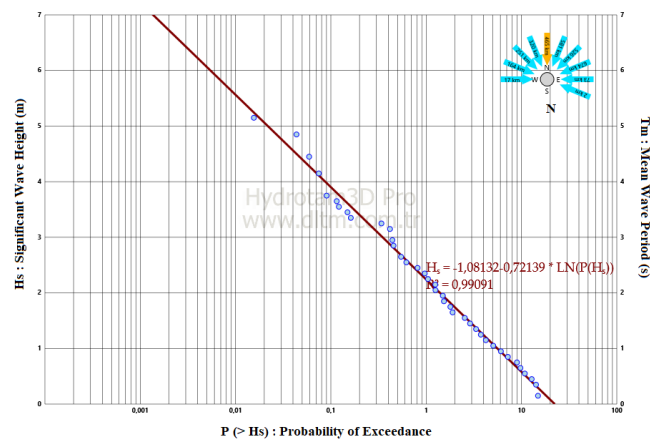


Figure 12. Long-term significant wave statistics for the North (N) direction

The results of the long-term wave statistics are presented in Figures 8-12. As part of the long-term wave statistics studies, the relationship between significant wave height (H_s) and mean wave period (T_m) for all directions is shown in Figure 13.

Table 2. The deep-sea significant wave height, mean wave period, breaking height, breaking depth, and breaking wavelengths for waves approaching the marine area

Approach Direction	Deep-sea significant wave height H_o (m)	Wave Period T(sec)	Deep Sea Wavelength L_o (m)	Breaking Wave Height H_b (m)	Wave Breaking Depth d_b (m)	Breaking Wavelength L_b (m)
NNW	5.45	7.53	88.37	5.04	6.37	54.99
NW	4.55	7.98	99.26	3.71	4.46	50.29
WNW	4.15	7.63	90.82	2,52	2.12	36.52

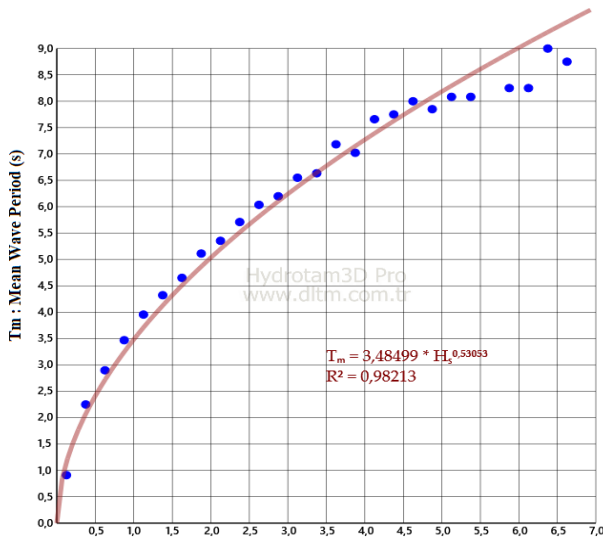


Figure 13. Long-term wave statistics: the relationship between significant wave height and mean wave period ($H_s - T_m$) (HYDROTAM-3D, 2023)

Annual and seasonal wave roses are presented in Figure 14, and monthly average and maximum significant wave heights are shown in Figure 15. When examining the long-term log-linear wave statistics studies, it is observed that the prevailing waves originate from the North (N) and East-northeast (ENE) directional ranges in the clockwise direction. The predominant directions are North (N) and Northeast (NE) in the winter and spring. The dominant wave direction during the summer is northeast (NE). In the autumn season, the dominant wave directions are Northeast (NE) and East-northeast (ENE) (Figure 14). While the monthly average wave height is at its highest, reaching 1 meter, the maximum significant wave heights vary in the 2.50-6.50 meters (Figure 15). In the long-term statistics, wind data from the ECMWF Operational Archive were utilized for the offshore point of the port. Figure 16 provides extreme (maximum) design wave values and non-exceedance probabilities obtained for specific recurrence periods for deep-sea highest wave heights over the years. As seen in Figure 16, for a 50-year return period ($R_p=50$ years return period), the significant deep-sea wave height (with a 90%

confidence interval) is $H_s=8.03$ meters, and the average wave period is $T_m=11.33$ seconds (HYDROTAM-3D, 2023).

The accuracy of HYDROTAM-3D has been assessed through comprehensive verification and validation studies, and the model has been applied to a wide range of applications in the last 20 years (Balas & Balas, 2023). Research has shown that HYDROTAM-3D has proved successful for a wide range of applications in real-life scenarios around the coast of Türkiye.

The HYDROTAM-3D is supported by Geographic Information Systems (GIS) and cloud computing, which facilitates processes such as data entry and output and remote access to all functions through a graphical user interface controlled by a menu structure. The model has a relational database for Turkish coastal waters that includes bathymetries of all Turkish coasts, hourly wind data since establishing Turkish Meteorological Stations (MS), and measured physicochemical data at the sites.

Based on long-term wave statistics in the marine area, the deep-sea significant wave height, mean wave period, breaking height, breaking depth, and breaking wavelengths for waves approaching from different directions are provided in Table 2.

In the marine area, the approximate depth of the wave-breaking zone is between the water depth of $d = -6.37$ meters and the shoreline.

The process of determining the height, period, and direction values of waves coming from deep-sea conditions, considering bathymetry and boundary conditions (islands, bays, capes), as well as the influence of coastal orientation, for sizing the structure to be designed is referred to as wave transformation. Wave transformation, or the process of obtaining the wave in front of the structure (wave transformation), was carried out to design the jetties planned at the mouth of Kabakoz Stream using the wave propagation module of the HYDROTAM 3D software (Balas & Balas, 2023) For the analysis, the bathymetry of the study area was initially loaded into the model (Figure 17).

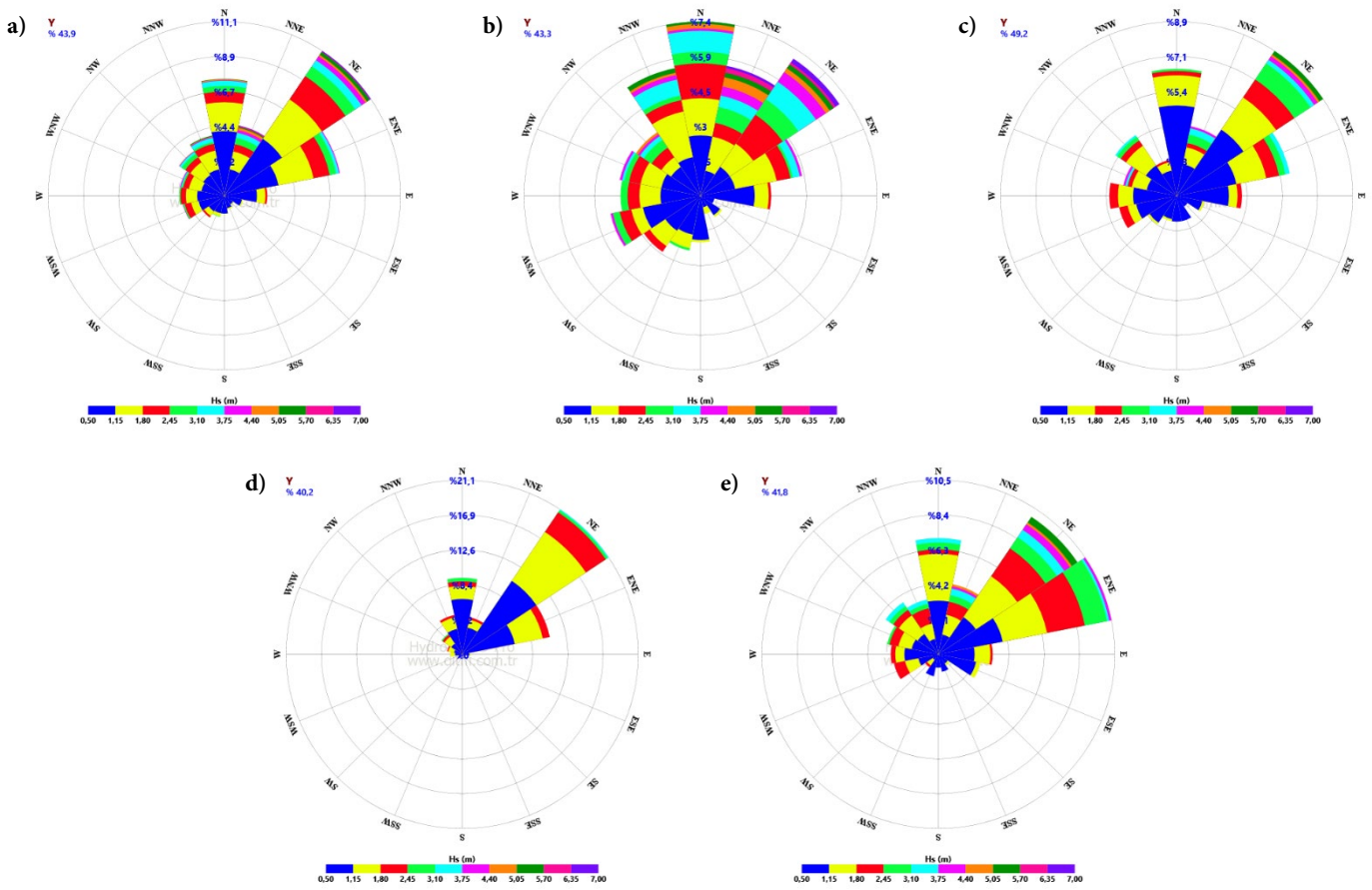


Figure 14. The project area's a) annual and seasonal (b: winter, c: spring, d: summer, e: autumn) wave roses (HYDROTAM-3D, 2023)

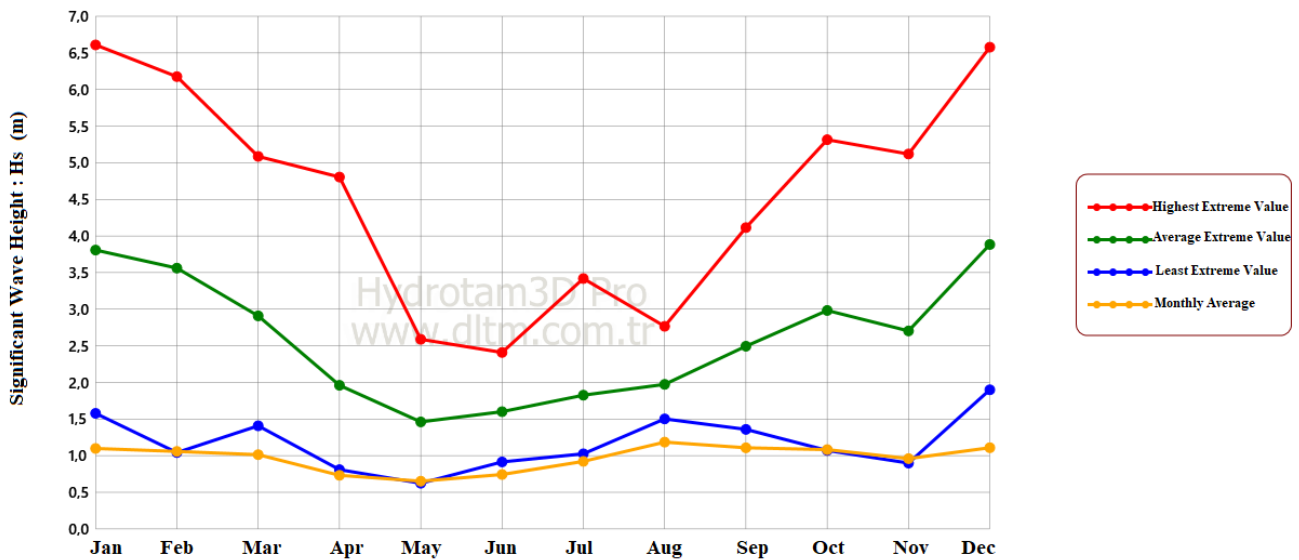


Figure 15. Monthly average and maximum significant wave heights (HYDROTAM-3D, 2023)

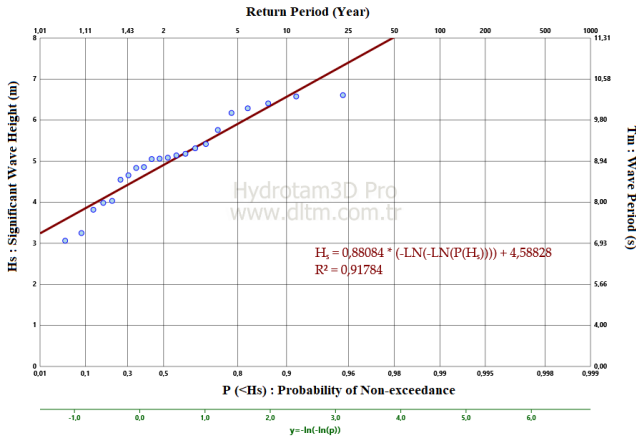


Figure 16. Extreme wave statistics (Gumbel Distribution) (HYDROTAM-3D, 2023)

The significant deep-water design wave height having a return period of $R_p=50$ years was obtained from the HYDROTAM3D wave climate module (Balas et al., 2023) with a 90% confidence interval as $H_s=8.03$ meters and an average wave period of $T_m=11.33$ seconds. The wave values obtained regionally because of the analysis are presented in Figure 16. The wave in front of the structure (design wave) was obtained using the HYDROTAM3D wave propagation module. The wave value at the structure's outermost point (crest), which should be formed at -2m according to the closure depth, was obtained as a model result. Solving the shallow-water slope equations with the HYDROTAM3D model transforms the

predicted wave heights in open waters into coastal areas under bathymetry and topography (Balas et al., 2023). Effects such as shoaling, refraction, diffraction, friction, breaking, and wave setup are calculated during wave propagation. Spatial or pointwise distribution maps of wave heights or temporal change graphs can be accessed. As a result, the Design Significant Wave Height in front of the structure was determined as $H_s=1.60$ meters, and the average wave period $T_m=4.65$ seconds (Figure 18).

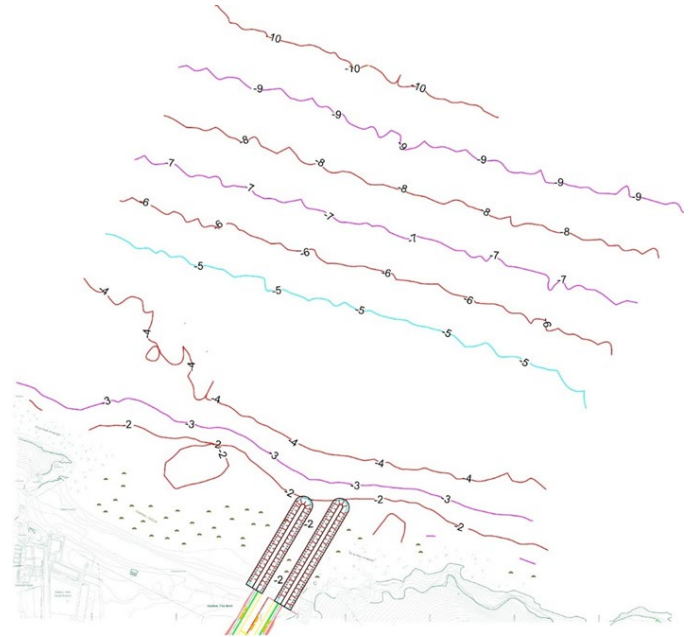


Figure 17. The bathymetry of the project area

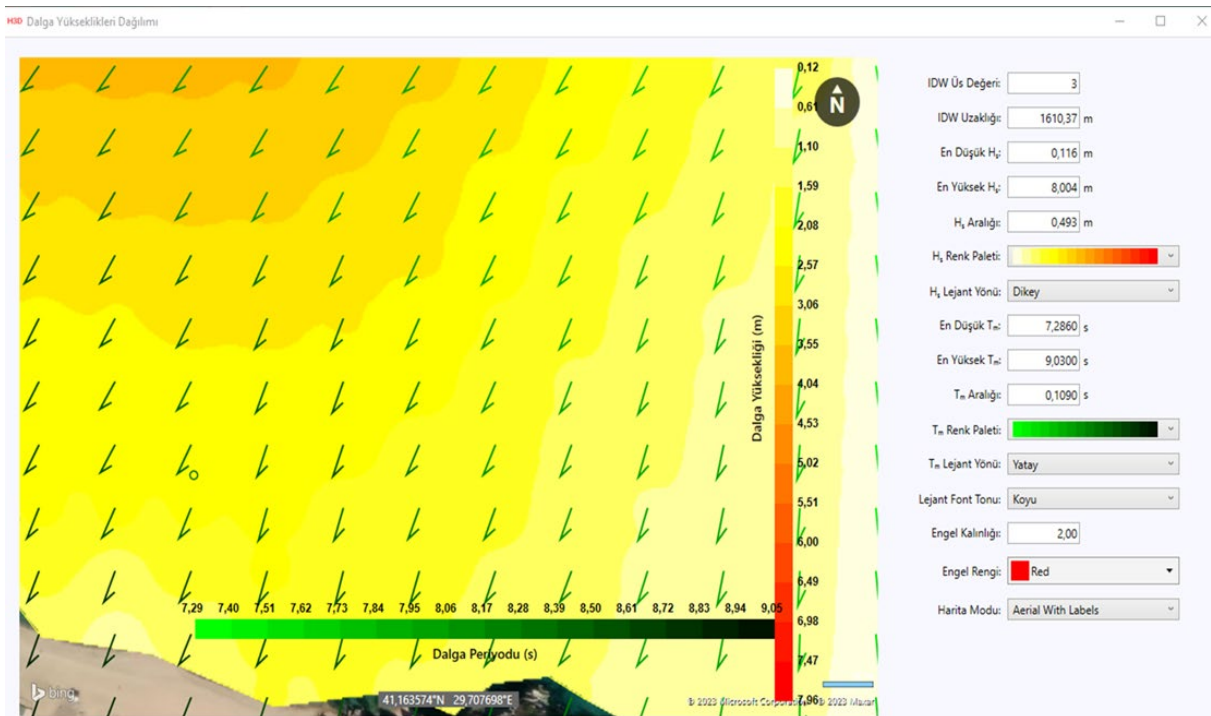


Figure 18. The study area's wave height (H_s) distributions (HYDROTAM-3D, 2023)

The closure depth was investigated to determine the distance from the outlet of the Kabakoz River jetty to the coastline. The closure depth is a theoretical depth along the beach profile where sediment transport does not occur, depending on wave height, period, and sediment grain size. Two equations by (Birkemeier, 1985; Hallermeier, 1981) are used to investigate the closure depth. Both equations use the significant wave height with a 12-hour annual exceedance probability.

Hallermeier closure depth equation (Hallermeier, 1981):

$$DoC = 2.28 * \frac{H_{12h}}{y} - 68.5 \left(\frac{H_{12h}^2}{g * T_{12h}^2 * y} \right) \quad (1)$$

Birkemeier closure depth equation (Birkemeier, 1985):

$$DoC = 1.75 * \frac{H_{12h}}{y} - 57.9 \left(\frac{H_{12h}^2}{g * T_{12h}^2 * y} \right) \quad (2)$$

The closure depths were investigated using the east (E) direction, which has the lowest wave height among the directions shown in Figure 8, and depths of -2.92 m according to the (Hallermeier, 1981) equation and -2.17 m according to the Birkemeier formula were obtained. The closure depth was determined based on these two formulas, and a value giving a shallower depth (Birkemeier) was selected to stay on the safe side. The deepest point of the structure was approximately set at -2.00 m, behind the closure depth as a result of these studies. In the event of a storm, the basin where the structure is seated, including the lower part, must be scanned to -2.00 m from the coast to the structure's end to eliminate the effect of stream-sea interaction and prevent sediment accumulation at the jetty mouth. This way, rebound effects will be prevented, and the risk of flooding will be mitigated. Following the modeling studies, jetty structures are proposed for the Kabakoz Stream in Figure 19, which will not affect the shoreline change. Closure depth is a theoretical depth along the beach profile where sediment transport does not occur, depending on wave height, period, and sediment grain size. The closure depth is the most important criterion in designing a structure that will not harm the coastal morphology. The hydraulic structure designed based on this value is presented in Figure 19.

The circulation in coastal water bodies is generally irregular and turbulent. The model connects turbulent and mean motion through vertical and horizontal eddy viscosities and mass exchange caused by vertical and horizontal eddy diffusions. In

coastal waters where the surface area of the water body, such as a gulf, is large compared to its depth, the turbulence intensity of the motion significantly varies in both horizontal and vertical directions. This difference in vertical and horizontal lengths creates a non-isotropic condition, making it crucial to use different eddy viscosity values in the model for both horizontal and vertical directions in simulations. By utilizing eddy viscosity values calculated with the isotropic k-ε model in the vertical direction, horizontal eddy viscosity values have been computed in the direction that compensates for this difference using a sub-turbulence model with a length scale in the horizontal direction. The seawater temperature, salinity, and density have been assumed to be constant spatially and throughout the depth.

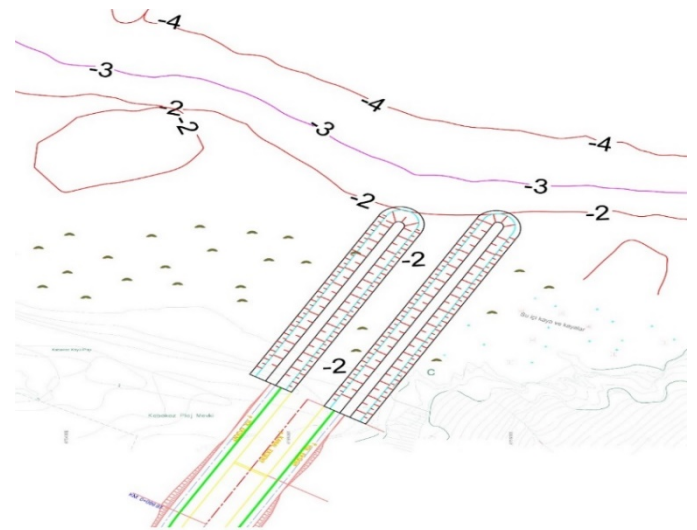


Figure 19. Designed jetty structure

A modeling study was conducted to determine the current pattern in the study's coastal area. 6-hour wind data was obtained from the ECMWF operational archive at coordinates 41.2°N-29.7°E for 2000-2022; 6-hourly annual current pattern time series were obtained. The current profile along the depth, obtained at the point where the depth of the jetty is approximately -2 m in the modeling area, is presented in Figure 20.

Coastal sediment transport analysis was conducted for the Kabakoz Beach segment based on the depth of breakwaters. Annual net and gross sediment volumes transported in different directions (m³/year) are presented in Figure 21. The annual sediment transport for Kabakoz Beach, which is approximately 300 meters long and bounded by rocky headlands from both east and west, is 367,821 m³/year. Due to the small and sheltered nature of the study area from both directions, the annual gross sediment transport does not reach

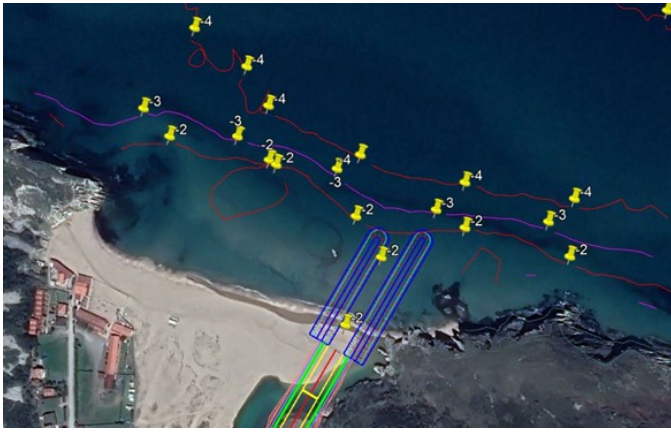


Figure 22. The locations of the newly constructed jetties and the direction of the coastline extension

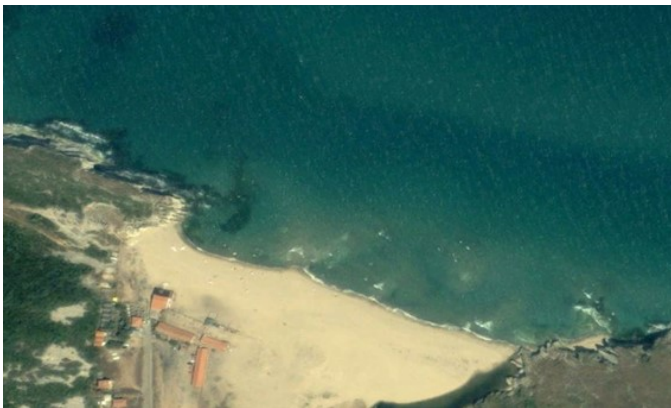


Figure 23. Satellite image of the jetty area's coastal morphology in 2003 (Google Earth, 2023)



Figure 24. Satellite image of the coastal morphology for the jetty area in the year 2021 (Google Earth, 2023)

The influence zone of the jetties has been determined to be approximately 60-80 m, as obtained from model analyses. After the completion of the construction of coastal structures, there is a limited change in coastal morphology due to the cessation of sediment transport in the E-W direction (Figure 25).

The HYDROTAM-3D model calculated directional wind waves based on long-term directional exceedance probabilities for coastal sediment transport quantities. The annual net coastal sediment transport quantity, Q_{net} , provides information

about the direction and amount of material accumulation or erosion along the coast. The total sediment quantity transported in one year, Q_{gross} , is used in studies to determine the effects of shoaling in navigation channels. The calculated net and total sediment quantities are provided in Table 3.

Table 3. Annual coastal sediment transport volume. Q ($m^3/year$)

Direction	ESE → WNW	WNW → ESE
N		103143.48
NNE	18208.82	
NE	135695.44	
ENE	63465.13	
E	3674.09	
ESE		
SE		
SSE		
S		
SSW		
SW		
WSW		
W		
WNW		3288.41
NW		13841.24
NNW		25964.43
Total	221043.49	146237.55
Net	74805.94	
Gross	367281.04	



Figure 25. The changes in coastal morphology occurred within two years based on the proposed coastal structure (HYDROTAM-3D, 2023)

In the study area, 146,237.55 m^3 of sediment is annually transported from west to east, and 221,043.49 m^3 is transported from east to west. In the absence of coastal structures, the sediment transport from east to west is approximately 1.5 times greater than the transport from west to east.

The annual net coastal sediment transport from east to west is estimated to be approximately 74,805.94 m³, while the total transport is estimated to be 367,281.04 m³. The expected changes in coastal morphology within two years, based on the proposed coastal structure modeled by HYDROTAM 3D, are presented in Figure 25.

The model predicts a maximum excavation of 3 m on the west side of the breakwater and a maximum accumulation of 3 m on the east side. According to the model results, the coast is expected to regain its sediment balance within approximately two years. Artificial nourishment with suitable granulometry material is recommended to counteract the changes occurring on the west side of the breakwater. The material used for nourishment should be compatible with the natural gradation of the shoreline. Crushed sand from a quarry can be used for this purpose. This way, nourishment with sand of appropriate granulometry can be transported to the excavation area, minimizing the impact of the structure on the coastline.

The Hudson formula based on the wave height obtained with the HYDROTAM3D software determined the armor layer stone category. A slope of 1/1.5 was chosen to align with the approved slope of the Kabakoz River reclamation project.

$$W_{50} = \frac{\gamma_s \cdot (H + \Delta MWL)^3 \cdot \tan \alpha}{(S_r - 1)^3 \cdot K_D} \quad (3)$$

W₅₀: Nominal armor weight (tons)

D_{n50}: Nominal median armor diameter = $\sqrt[3]{\frac{W_{50}}{\gamma_s}}$ (m)

γ_s: Unit weight of rock = 2.65 t/m³

γ_w: Unit weight of seawater = 1.025 t/m³

tan α: Slope of the structure = 1/1.5

H_d: Design significant wave height of 1.60 m

K_{D, breaking}: Stability coefficient of Hudson for wave breaking condition= 1.9

S_r: Specific weight of armor= (γ_s / γ_w - 1) = 1.58

The HYDROTAM-3D modeling results indicate the highest and lowest water level changes according to RCP8.5, expected to occur above the TUDES average water level (MWL). The RCP8.5 Sea Level Rise (ΔMWL) expected in 100 years is estimated to be 87 cm. The cumulative scenario value includes wind setup, tidal effect, and wave setup. The nominal stone diameter was determined as D_{n50}= 0.70 m, and the protective layer thickness was selected as 2-4 t. The thickness of the layer, which will be constructed in two rows, is 2.00 m. A single layer of 0.4 - 2 tons will be used as the filter layer. The layer thickness for a single row is 0.75 m. It is deemed suitable for design and construction to use material weighing 0 - 0.4 tons at an

elevation of +0.50 for the core layer. It is designed with a width of 3.50 m at its narrowest point to allow for construction. The cross-section of the jetty type is presented in Figure 26, and the designed coastal structure at the river mouth is shown in Figure 27.

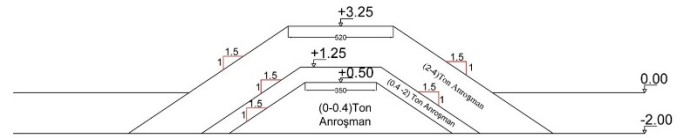


Figure 26. Cross-section of jetty

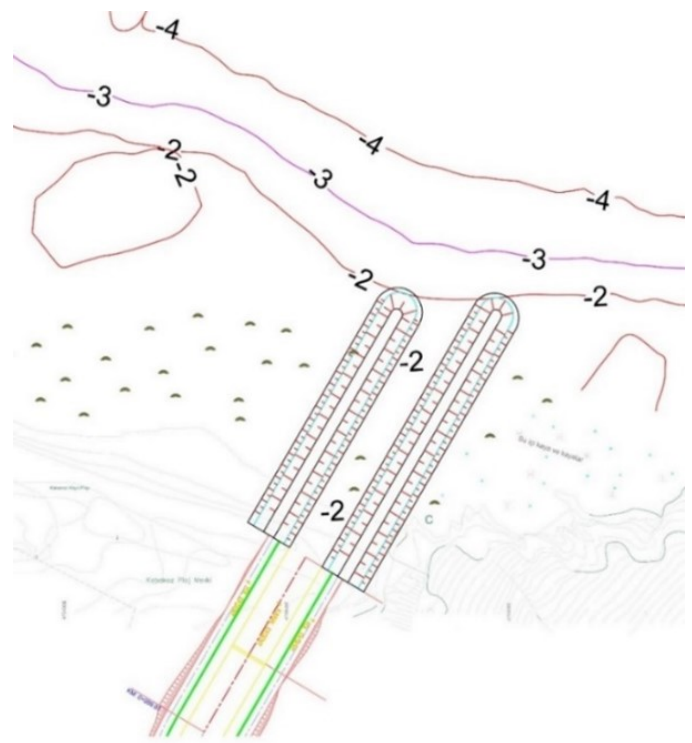


Figure 27. Designed jetty

Monte Carlo simulation is applied to model the probability of different outcomes in design that cannot easily be predicted due to the intervention of random variables (Balas, 2023). Monte Carlo simulation is used to understand the effects of risk and uncertainty on environmental parameters (Durap et al., 2023). Hence, the Monte Carlo simulation will ultimately be fruitful for the probabilistic design of coastal structures. Predicting uncertainties such as wave height is the most crucial part of coastal structure design. In the scope of this paper, a probabilistic design is also conducted for the jetty, which will be constructed on the outlet of the Kabakoz River, and the results are compared with a deterministic design. The Hudson equation is the limit state function, and random variables are modeled by various probability distributions in Monte Carlo Simulation, as seen in Table 4. 30000 simulations are conducted for randomly generated samples.

Table 4. The variations of design parameters and probability distributions modeled in MCS (SD: Standard deviation)

Variable	Definition	Minimum	Average	Maximum	SD	Distribution type	Distribution
W50	Median Armor Weight (tons)	0.40	0.7	1.50	0.20	Simulated	
H _d	Design Wave Height	1.30	1.60	1.90	0.10	Normal	
ΔMWL	Mean Sea Level Rise	0.71	0.87	1.12	0.05	Normal	
γ _s	Unit weight of Armor	2.50	2.65	2.80	0.05	Normal	
γ _w	Unit Weight of water	1.01	1.025	1.04	0.01	Normal	

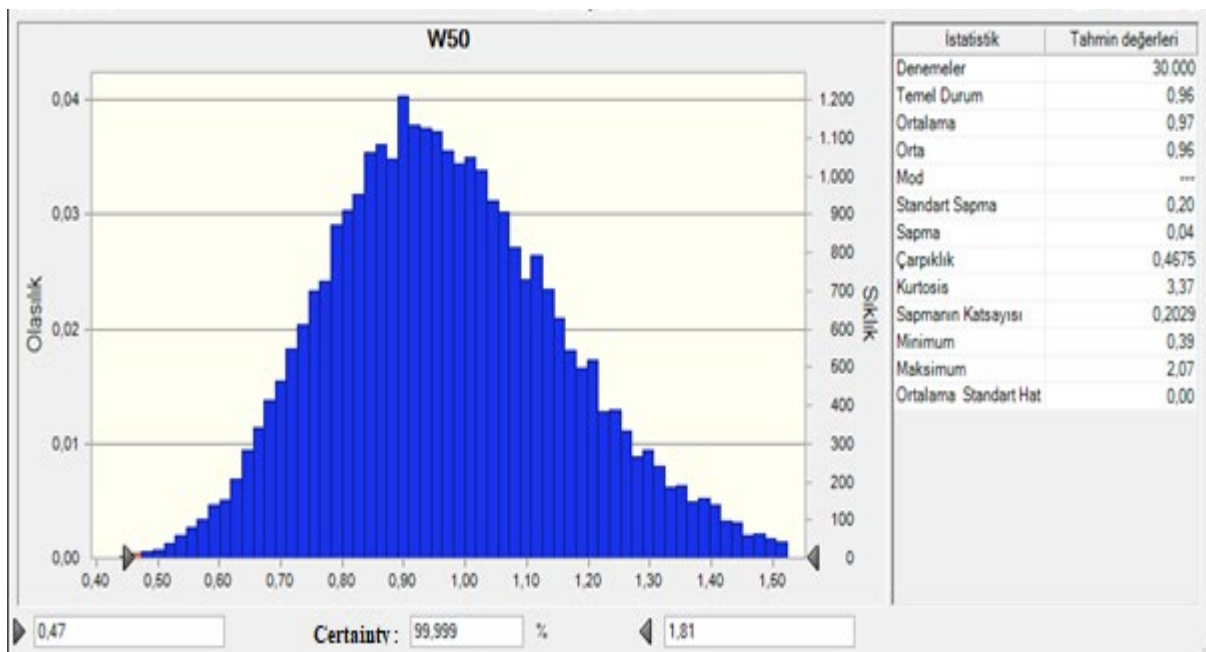


Figure 28. Hudson limit state function (W50) of the structure failure in its lifetime

The result of the Monte Carlo Simulation for Hudson limit state function (W_{50}) indicates the structure’s failure in its lifetime of 50 years, as shown in Figure 28. As can be seen from the figure, the lifetime failure probability of the coastal structure is 10^{-3} when considering all the environmental risk parameters, such as climate change and sea level changes.

Following the completion of simulations, design parameters of paramount importance were identified through a sensitivity analysis, as seen in Figure 29. It is seen in the figure that H_{design} has the greatest contribution to the determination of structural stability concerning MCS. The sensitivity analysis is applied to analyze the contribution of random design variables in the Monte Carlo simulation (MCS).

One of the goals of this study is to determine the correlation between various design variables. The scatter diagrams in Figure 30 show that the coastal structure’s stability is positively

or negatively correlated with design variables. The design significant wave height (H_d) affects the limit state function with a maximum correlation of $\rho=0.918$, indicating the limit state function is highly sensitive to the deviations and uncertainties in design wave height. The unit weight of seawater (γ_w) has a moderately low effect on stability with a correlation of $\rho=0.1052$. Unit weight of rock has a negative effect over stability with $\rho=-0.35$.

The results of this study show the precision of probabilistic design while it takes environmental risk parameters such as climate change and sea level changes. The deterministic method does not consider environmental effects; thus, the general approach for designing coastal structures is insufficient. The first investment costs of coastal structures are high and hard to construct. For this reason, the probabilistic method should become an indispensable part of coastal structures design.

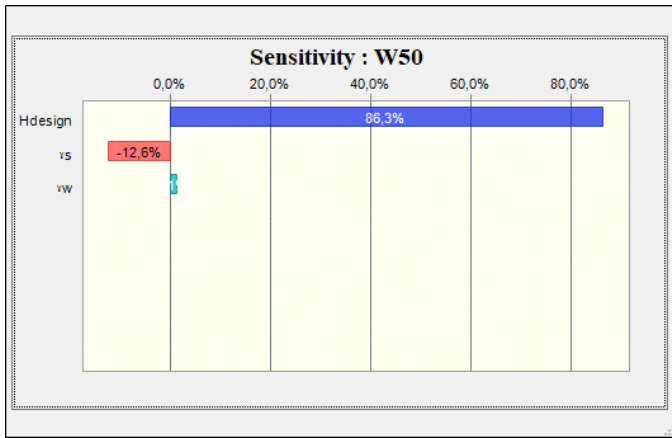


Figure 29. The sensitivity analysis of Hudson limit state function conducted by MCS

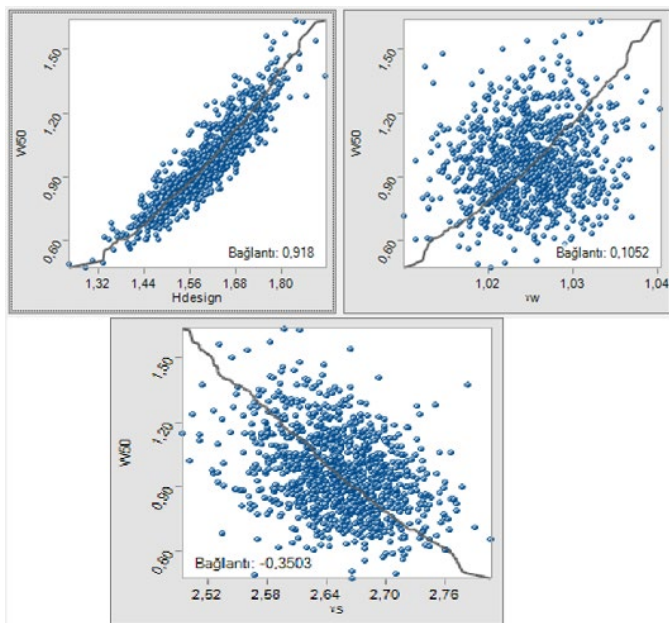


Figure 30. Scatter diagrams of design parameters

Discussion

Hourly wind measurements from the Şile Meteorological Station and 6-hour wind forecasts from the ECMWF operational archive at 41.2°N-29.7°E, representing the study area, were compared and examined. Comparisons of wind speeds for common measurement periods and durations of the data sources are presented in Figure 3. All presented wind speed measurements and forecasts are at a height of 10 m (U_{10}). After the comparison studies, it was decided that ECMWF wind forecasts over the sea for the coordinates 41.2°N-29.7°E between 2000-2021 can be safely used to determine the wind climate of the coastal area in the study region. The wind rose for ECMWF coordinates 41.2°N-29.7°E is presented in Figure 4.

When examining the wind rose study, it is observed that the wind blows from the northeast (NE) to the east-east (ENE)

direction in the clockwise direction from the sea. An increase in the frequency of Southwest (SW) winds blowing from the land is observed in the winter and spring seasons, while in the summer and autumn seasons, the frequency of Northeast (NE) winds increases. Monthly average and maximum wind speeds are also presented graphically (see Figure 5). Monthly average wind speeds are calculated by taking the arithmetic average of all wind speeds within that month. The monthly maximum values represent the highest, lowest, and average maximum values observed during the same periods within that month (the average of the highest values for each year for any given month). The highest wind speeds and directions by year are presented in Figure 6. The monthly average wind speed ranges between 4-5 m/s, while the highest maximum wind speeds vary between 12-18 m/s. Throughout the study period, the highest wind speed was observed at 18 m/s, blowing from the North (N) direction. The long-term wind statistics follow the Weibull probability distribution for dominant wind directions.

From the extreme value (Gumbel Distribution) wind statistics, the wind speed with a recurrence period of twenty-five hours per year is obtained as $V_s=18.718$ m/s with a 90% confidence interval of ± 0.172 m/s.

Long-term wave statistics studies were conducted using wave predictions from the ECMWF operational archive for the coordinates 41.2°N - 29.7°E from 2000-2022. The significant wave height ($H_{s,12}$) obtained from long-term wave statistics studies has a range of $1.66 \text{ m} < H_{s,12} < 5.47 \text{ m}$, with a 12-hour-per-year exceedance probability. According to the Coastal Structures Planning and Design Technical Principles of the Ministry of Transport and Infrastructure (2016) document, it falls under the effective coast (E) classification based on wave height. Model predictions also indicate that the primary wave direction is clockwise from North (N) to Northeast (NE). The results of long-term wave statistics are presented in Figure 7.

As part of the long-term wave statistics studies, the relationship between significant wave height (H_s) and mean wave period (T_m) for all directions is shown in Figure 13. Annual and seasonal wave roses are presented in Figure 14, and monthly average and maximum significant wave heights are provided in Figure 15. When examining long-term log-linear wave statistics, it is observed that the dominant waves come from the North (N) and East-Northeast (ENE) directions in a clockwise direction. The dominant directions are North (N) and Northeast (NE) in the winter and spring. The prevailing wave direction in the summer is Northeast (NE). In the autumn season, the dominant wave directions are Northeast (NE) and East-Northeast (ENE) (Figure 14). The monthly average wave

height is 1 m, while the highest significant wave heights vary between 2.50 and 6.50 m (Figure 15). In the long-term statistics, ECMWF Operational Archive wind data were used for the point offshore of the jetty. Figure 16 provides extreme (maximum value) design wave values and non-exceedance probabilities obtained for certain return periods from deep-sea highest wave heights by years. As seen in Figure 16, for a return period of 50 years ($R_p=50$ years recurrence interval), the significant deep-sea wave height (at a 90% confidence level) is $H_s=8.03$ m, and the average wave period is $T_m=11.33$ seconds. The process of determining the height, period, and direction values of waves coming from deep-sea conditions, reaching the structure front due to bathymetry and boundary conditions (islands, bays, headlands), and the effect of coastline orientation is obtained as a result of the wave transformation model.

Wave transformation (obtaining the structure front wave) for the jetties design planned at the Kabakoz Stream sea outlet was conducted using the wave propagation module of the HYDROTAM3D software. For the analysis, the bathymetry of the project area was first loaded into the model. The wave in front of the structure (design wave) was obtained using the HYDROTAM3D wave propagation module. The wave value at the outermost point (toe) of the structure, which should be formed at a closure depth of -2m, was obtained from the model results. The HYDROTAM3D model (HYDROTAM-3D, 2023) solves the shallow water equations to transfer the predicted wave heights in the open sea to coastal areas under the influence of bathymetry and topography. Wave progression involves calculations of shoaling, refraction, diffraction, friction, breaking, and wave setup effects. Spatial or pointwise distribution maps of wave heights and temporal variation graphs can be accessed. Regionally obtained wave values are presented in Figure 18. As a result, the design's significant wave height, $H_s=1.60$ m, and average wave period, $T_m=4.65$ seconds, are obtained in the structure front, considering the water depth. The breaking index is approximately 0.8, close to the 0.78 breaking index, confirming the model result. As a result of these studies, the deepest point of the structure has been placed at a depth of approximately 2.00 meters, ensuring that it remains below the closure depth. In storms, to eliminate the effect of stream-sea interaction and prevent sediment accumulation at the mouth of the jetty, the basin where the structure is placed, including the lower section, needs to be dredged to -2.00 meters from the coast to the structure's end. The dredging will prevent backflows and mitigate the risk of flooding.

In conclusion, in the study area, $146,237.55$ m³ of sediment is transported annually from west to east and $221,043.49$ m³

from east to west. In the absence of coastal structures, sediment transport from east to west is approximately 1.5 times greater than from west to east. The annual net coastal sediment transport from east to west is approximately $74,805.94$ m³, while the total transport is estimated to be $367,281.04$ m³. The expected changes in coastal morphology within two years, based on the proposed coastal structure modeled by HYDROTAM 3D, are presented in Figure 25. The lengths of the jetties are approximately the same as the rocky headlands in Kabakoz Beach, which is bounded by two rocky headlands. Kabakoz Beach, located between the rocky headlands, is a well-protected beach with sediment movement along approximately a 300 m coastal stretch, as indicated by the model results. The coastline is expected to reach sediment balance within approximately two years.

The sediment transport, influenced by parameters such as breaking depth, bathymetry, coastal sediment grain size, structure location and dimensions, and closure depth, is predicted to have a maximum erosion of 3 m on the west side of the jetty and a maximum accumulation of 3 m on the east side, according to the model results. The influence area of the jetties is obtained to be approximately within the range of 60-80 m after model analyses. Using artificial nourishment with suitable granulometry in the expected eroded shore sections is recommended. The material used in nourishment should be compatible with the natural gradation of the shore. Crushed sand obtained from a quarry can be used for this purpose. Thus, by transporting sand with the appropriate grain size to the eroded area, the impact of the structure on the coastline can be minimized.

The most crucial part of this study is its difference from conventional methods, as the developed methodology can include the future environmental changes due to global warming. This aspect provides researchers or designers with the most reliable design of coastal structures such as rubble mounds or piles, allowing the alteration of design codes considering the changes in future environmental parameters.

Conclusion

Using the Integrative Probabilistic Design Approach of River Jetties introduced in this paper, 3D numerical models were used for the design considering the sediment transport near the jetties. As a result, the optimum layout and design of jetty structures were obtained by the proposed "Integrative Probabilistic Design Approach" and are presented in Figure 19 for the Kabakoz River. This optimum layout and design will not

interfere with the coastline long-term, balancing the environmental effects.

Closure depth is a theoretical depth along the beach profile where sediment transport does not occur, depending on wave height, period, and sediment grain size. Closure depth is the most important criterion in designing a structure that will not damage coastal morphology. The hydraulic structure designed based on this value is presented in Figure 27. Due to the east-southeast to west-northwest (ESE-WNW) direction of sediment transport, erosion will occur in the influence area of the western jetty. Since the eastern jetty is planned to be constructed in the region where the rocky area begins, it will not effectively impact long-term sediment transport.

Additionally, the lengths of the jetties are approximately the same as the rocky headlands in Kabakoz Beach, which is bounded by two rocky headlands. Kabakoz Beach is a well-protected beach between the rocky headlands, with sediment moving along approximately a 300 m coastal stretch. According to the model results, the coastline is expected to reach a sediment balance within approximately two years. After the completion of the construction of coastal structures, limited changes in coastal morphology are expected due to the termination of E-W sediment transport, as shown in Figure 25. The calibration of the model was examined for the change in the old-new coastline from 2003 to 2021, as shown in s 26. As evident from the figures, the coastline is in balance within itself. The proposed jetties will be constructed at the easternmost part of the coast, at the end of the rocky headland, so the impact of the jetties on coastal morphology will be extremely limited in the long term.

In conclusion, Monte Carlo Simulation (MCS) is applied to model the probability of different outcomes in a process that cannot be easily predicted due to the intervention of random variables. Thirty thousand simulations were conducted for randomly generated samples, as seen in Table 4. MCS gave the lifetime failure probability of the coastal structure as 10^{-3} , which means the structure is reliable under the effect of risk parameters such as sea level increase due to climate change changes when the design standards are considered.

The consequences of failure give the target reliability as in (British Standards, 2005), where values are conferred for the target reliability. (Det Norske Veritas (DNV), 1992) developed a more specific code for marine structures in 1992, where the target reliability is 10^{-3} for structures with less serious failure consequences, and this validated the model developed in this paper. The class of failure depends on the possibility of timely warning as the development of failure. These codes and

standards are used as a first estimate and guidance for the design of maritime structures. The precise design can be performed using the methodology developed in this paper. The reliability of the structure is evaluated by the model and compared with the target reliability suggested by the standards. These standards do not consider the effects of climate change yet.

This study has powerful outcomes in designing robust coastal structures and precisely predicting shoreline change while providing the basis for design codes such as Det Norske Veritas. The probabilistic design presented in this paper's scope is the most reliable way to achieve this success. This method can be used to alter the regulations to reduce costs and design robust structures.

Recommendation for Future Research

For future studies, it is recommended to develop the following items to improve the model presented in this paper:

1. It is recommended that the low-resolution outputs of the climate models included in the IPCC's CMIP6 protocol be obtained by dynamically reducing them to grid points with a resolution of approximately 1 km, creating the initial and boundary conditions required for the hydrodynamic modeling.
2. The combined effect of climate change and sea level rise is expected to be much greater for marine structures when the structural risks are incorporated into the reliability model.
3. It is possible in the model to modify the risk iteratively according to its environmental consequences based on the scenario by considering the hazard to the marine environment. Hence, the probability of earthquakes and tsunamis can be added to the structural reliability model.

Acknowledgements

The authors would like to thank Dr. Saleh Abdalla from the Reading (UK) headquarters of ECMWF (European Centre for Medium-Range Weather Forecasts) and DLTM Software Technologies at the Gazi University Technopark for their permissions granted in the application of HYDROTAM-3D in modeling and the database that supports the findings of this study. This research received no specific grant from any funding agency.

Compliance With Ethical Standards

Authors' Contributions

AU: Conceptualization, Methodology, Software, Validation, Formal analysis, Investigation, Resources, Data Curation, Writing—Original Draft
CEB: Writing—Review & Editing, Supervision, Visualization
All authors read and approved the final manuscript.

Conflict of Interest

The authors declare that there is no conflict of interest.

Ethical Approval

For this type of study, formal consent is not required.

Funding

Not applicable.

Data Availability

The data supporting this study's findings are available from HYDROTAM-3D. However, restrictions apply to the availability of these data, which were used under license for the current study and are not publicly available. Data are, however, available from the authors upon reasonable request and with permission of HYDROTAM-3D (<http://www.hydrotam.com/>) and ECMWF (<https://www.ecmwf.int/>)

References

- AYGM. (2016). Kıyı Yapıları Planlama ve Tasarım Teknik Esasları. Retrieved on January 3, 2024, from <https://aygm.uab.gov.tr/uploads/pages/kiyi-yapilari-planlama-ve-tasarim-teknik-esaslari/teknikesas.pdf>
- Balas, E. A., & Balas, L. (2023). Wind and wave climate modelling in coastal waters. In O. Erkman & G. Gafurova (Eds.), *Proceedings of the 9th International Zeugma Conference on Scientific Research* (pp. 1133–1148). İKSAD Publishing House.
- Balas, E. A. (2023). A hybrid Monte Carlo simulation risk model for oil exploration projects. *Marine Pollution Bulletin*, 194(A), 115270. <https://doi.org/10.1016/j.marpolbul.2023.115270>
- Balas, E. A., Yıldırım, P. F., & Balas, L. (2023). Water quality management system and modeling in coastal waters. In Y. B. Ergen, M. Cojocar, & I.-A. Drobot (Eds.), *Proceedings of the 8th International Asian Congress on Contemporary Sciences* (pp. 153–164). Institute of Economic Development and Social Research Publications.
- Balas, L. (2022). Hydrotam 3D Modeli. <https://denam.gazi.edu.tr/view/page/41310/hydrotam-uc-boyutlu3d-sayisal-hidrokinamik-ve-tasinim-modeli>
- Birkemeier, W. A. (1985). Field data on seaward limit of profile change. *Journal of Waterway, Port, Coastal, and Ocean Engineering*, 111(3), 598–602. [https://doi.org/10.1061/\(ASCE\)0733-950X\(1985\)111:3\(598\)](https://doi.org/10.1061/(ASCE)0733-950X(1985)111:3(598))
- British Standards. (2005). Eurocode 1: Actions on structures. Det Norske Veritas (DNV). (1992). Structural reliability analysis of marine structures.
- Durap, A., Balas, C. E., Çokgör, Ş., & Balas, E. A. (2023). An integrated bayesian risk model for coastal flow slides using 3-D hydrodynamic transport and Monte Carlo simulation. *Journal of Marine Science and Engineering*, 11(5), 943. <https://doi.org/10.3390/jmse11050943>
- Franzen, M. O., Fernandes, E. H. L., & Siegle, E. (2021). Impacts of coastal structures on hydro-morphodynamic patterns and guidelines towards sustainable coastal development: A case studies review. *Regional Studies in Marine Science*, 44, 101800. <https://doi.org/10.1016/j.rsma.2021.101800>
- Google Earth. (2023). <https://earth.google.com/web>
- Hallermeier, R. J. (1981). A profile zonation for seasonal sand beaches from wave climate. *Coastal Engineering*, 4(3), 253–277. [https://doi.org/10.1016/0378-3839\(80\)90022-8](https://doi.org/10.1016/0378-3839(80)90022-8)
- HYDROTAM-3D. (2023). HYDROTAM-3D, Three dimensional hydrodynamic transport and water quality model (6.3). <http://www.hydrotam.com/>
- Lima, M., Coelho, C., Veloso-Gomes, F., & Roebeling, P. (2020). An integrated physical and cost-benefit approach to assess groins as a coastal erosion mitigation strategy. *Coastal Engineering*, 156, 103614. <https://doi.org/10.1016/j.coastaleng.2019.103614>
- Phanomphongphaisarn, N., Rukvichai, C., & Bidorn, B. (2020). Impacts of long jetties construction on shoreline change at the western coast of the Gulf of Thailand. *Engineering Journal*, 24(4), 1–17. <https://doi.org/10.4186/ej.2020.24.4.1>
- Roebeling, P., d'Elia, E., Coelho, C., & Alves, T. (2018). Efficiency in the design of coastal erosion adaptation strategies: An environmental-economic modelling approach. *Ocean & Coastal Management*, 160, 175–184. <https://doi.org/10.1016/j.ocecoaman.2017.10.027>
- Setyandito, O., Purnama, A. C., Yuwono, N., Juliastuti, J., & Wijayanti, Y. (2020). Shoreline change with groin coastal protection structure at North Java Beach. *ComTech: Computer, Mathematics and Engineering Applications*, 11(1), 19–28. <https://doi.org/10.21512/comtech.v11i1.6022>
- Wamdi Group. (1988). The WAM Model—A third generation ocean wave prediction model. *Journal of Physical Oceanography*, 18(12), 1775–1810. [https://doi.org/10.1175/1520-0485\(1988\)018<1775:TWMTGO>2.0.CO;2](https://doi.org/10.1175/1520-0485(1988)018<1775:TWMTGO>2.0.CO;2)